Biochimica et Biophysica Acta 1852 (2015) 2504–2516

Contents lists available at ScienceDirect

Biochimica et Biophysica Acta

journal homepage: www.elsevier.com/locate/bbadis

Epigenetic landscape in PPARγ2 in the enhancement of adipogenesis of mouse osteoporotic bone marrow stromal cell☆

Yongxing Zhang [a,1], Chao Ma [b,1], Xuqiang Liu [c,1], Zhenkai Wu [d], Peng Yan [a], Nan Ma [e], Qiming Fan [f,*], Qinghua Zhao [a,*]

[a] Department of Orthopaedics, Shanghai First People's Hospital, School of Medicine, Shanghai JiaoTong University, Shanghai 200080, PR China
[b] Department of Spine Surgery, XuZhou Central Hospital, XuZhou, JiangSu 221009, PR China
[c] Department of Orthopaedics, First Affiliated Hospital of Nanchang University, Nanchang, Jiangxi Province 330019, PR China
[d] Department of Pediatric Orthopaedics, Shanghai XinHua Hospital, School of Medicine, Shanghai JiaoTong University, Shanghai 200092, PR China
[e] Department of Cardiac Surgery, University of Rostock, Schillingallee 35, Germany
[f] Shanghai Key Laboratory of Orthopedic Implants, Department of Orthopedic Surgery, Shanghai Ninth People's Hospital, Shanghai JiaoTong University School of Medicine, Shanghai 200011, PR China

ARTICLE INFO

Article history:
Received 25 May 2015
Received in revised form 21 August 2015
Accepted 24 August 2015
Available online 28 August 2015

Keywords:
Osteoporosis
PPARγ
Adipogenesis
Epigenetics
Bone marrow stromal cells
β-Catenin

ABSTRACT

Osteoporosis is one of the most prevalent skeletal system diseases; yet, its pathophysiological mechanisms remain elusive. Adipocytes accumulate remarkably in the bone marrow of osteoporotic patients. The potential processes and molecular mechanisms underlying adipogenesis in osteoporotic BMSCs have attracted significant attention as adipocytes and osteoblasts share common precursor cells. Some environmental factors influence bone mass through epigenetic mechanisms; however, the role of epigenetic modifications in osteoporosis is just beginning to be investigated, and there is still little data regarding their involvement. In the current study, we investigated how epigenetic modifications, including DNA methylation and histone modifications, lead to adipogenesis in the bone marrow during osteoporosis. A glucocorticoid-induced osteoporosis (GIO) mouse model was established, and BMSCs were isolated from the bone marrow. Compared with normal BMSCs, osteoporotic BMSCs had significantly increased adipogenesis potential and decreased osteogenesis potential. In osteoporotic BMSCs, PPARγ2 regulatory region DNA hypo-methylation, histone 3 and 4 hyper-acetylation and H3K9 hypo-di-methylation were observed. These epigenetic modifications were involved not only in PPARγ2 expression but also in osteoporotic BMSC adipogenic differentiation potential. We also found that Wnt/β-catenin signal played an important role in the establishment and maintenance of epigenetic modifications at PPARγ2 promoter in osteoporotic BMSCs. Finally, we inhibited adipogenesis and rescued osteogenesis of osteoporotic BMSCs by modulating those epigenetic modifications. Our study provides a deeper insight into the pathophysiology of osteoporosis and identifies PPARγ2 as a new target for osteoporosis therapy based on epigenetic mechanisms.

1. Introduction

Osteoporosis is one of the most prevalent skeletal system diseases and it is estimated to affect approximately 30% of women and 12% of men over 50 years of age [18]. It is characterized by a decrease in bone mass and microarchitectural changes in bone tissue that lead to an attenuation of bone resistance and susceptibility to fracture. The pathogenesis of the disease remains hitherto elusive, resulting in augmented interest in basic and clinical research into the mechanisms of osteoporosis. Osteoporosis research initially focused on osteoclastic activity and bone resorption processes, and then on osteoblastogenesis. More recently, the differentiation potential of bone marrow stromal cells (BMSCs) has become an area of intense interest [31].

BMSCs are multipotent as they able to differentiate into osteoblasts, chondrocytes, adipocytes, and/or myocytes in vitro and following in vivo implantation. As BMSCs are the shared precursor cells for osteoblasts and adipocytes, a reciprocal relationship between osteogenesis and adipogenesis was previously postulated [25]. The fat theory for osteoporosis postulates that the balance between these cell types is always impaired in bone marrow from osteoporosis patients, with adipogenesis overwhelming osteogenesis to upset BMSC activity and the

☆ Author contributions: Yongxing Zhang: Collection and/or assembly of data, data analysis and interpretation; Chao Ma: collection and/or assembly of data, data analysis and interpretation; Xiuqiang Liu: collection and/or assembly of data, data analysis and interpretation; Zhenkai Wu: collection and/or assembly of data; Peng Yan: collection and/or assembly of data; Nan Ma: conception and design; Qi-ming Fan: conception and design, financial support, data analysis and interpretation, and manuscript writing; and Qing-hua Zhao: conception and design, financial support, data analysis and interpretation, and manuscript writing.

* Corresponding authors.
E-mail addresses: chillow@163.com (Q. Fan), sawboneszhao@163.com (Q. Zhao).
[1] These authors contributed equally to this work.

http://dx.doi.org/10.1016/j.bbadis.2015.08.020
0925-4439/

microenvironment [19,26]. Furthermore, this imbalance is also observed in other physiological and pathological conditions, such as aging, microgravity, immobilization, ovariectomy, diabetes, and glucocorticoid overdose [19,43]. The possibility of inhibiting BMSC adipogenesis opens new avenues for osteoporosis therapy; however, why BMSC adipogenesis overwhelms osteogenesis in osteoporosis is currently unknown.

Adipogenic differentiation is a complex process in which concerted gene expression is precisely regulated by various adipogenic factors. Among these factors, peroxisome proliferator-activated receptor γ (PPARγ) and CCAAT/enhancer binding protein α (C/EBPα) play central roles controlling many downstream adipogenic genes [6]. PPARγ, a member of the hormone nuclear receptor superfamily, is the only gene that is sufficient to activate adipogenesis on its own [36,37]. PPARγ has two isoforms, PPARγ1 and PPARγ2; the latter has been shown to be an adipocyte specific isoform and is more efficient than PPARγ1 in promoting adipocyte differentiation. PPARγ2 contains an additional 30 amino acids at its N-terminus, that are not present in PPARγ1, thus indicating that the transcription of each isoform is initiated at different start sites, and that it is differentially controlled. At the onset of adipogenesis, C/EBPβ and C/EBPδ are quickly induced and subsequently cooperate to activate PPARγ and C/EBPα expression to promote terminal adipogenesis [2,41]. Investigating PPARγ's role in osteoporotic BMSC adipogenesis and how it is modulated in osteoporotic BMSCs could provide a deeper insight into osteoporosis pathophysiology and highlight PPARγ as a target gene for osteoporosis prevention or treatment.

There is no doubt of the importance of genetic factors in osteoporosis. Some cases of osteoporosis resulting from gene mutations have been reported [23]; however, most cases involve multiple genes, with no single gene being responsible for the entire osteoporotic phenotype. Osteoporosis is likely to involve complex gene–gene and gene–environment interactions. Some environmental influences that have been shown to be important osteoporosis risk factors deserve much more attention. Given the high stability of the genome, environmental factors generally influence genome activity via mechanisms that do not alter the DNA sequence. Some of these mechanisms are defined as epigenetic mechanisms, which are inherited through generations and cell divisions but do not alter the DNA sequence.

Epigenetic mechanisms include DNA methylation, histone modifications and miRNAs [3]. DNA methylation and histone modification modulate gene expression at the level of transcription while miRNAs exert their effects at the post-transcriptional level. The most widely studied epigenetic mark is DNA methylation, especially in oncogenesis. DNA methylation is generally associated with transcriptional silencing. Histone modifications, including methylation, acetylation, phosphorylation, SUMOylation and ubiquitination, have also been widely investigated [10,30]. The effects of histone modifications are somewhat complicated, as they depend not only on the type of histone modified but also on the type and number of chemical groups that are added. In general, histone modifications can be divided into two groups: those that are associated with transcriptional activation (acetylation and phosphorylation) and those that are associated with transcriptional repression (methylation, ubiquitination and sumoylation) [27].

The involvement of epigenetic modifications in osteoporosis is just beginning to be investigated, and data regarding its role in osteoporosis is scarce. In the current study, a glucocorticoid-induced osteoporosis (GIO) mouse model was established and BMSCs were isolated from the bone marrow. Compared with normal BMSCs, osteoporotic BMSCs had significantly enhanced adipogenic differentiation potential as well as PPARγ2 regulatory region DNA hypo-methylation, histone 3 and 4 hyper-acetylation, and H3K9 hypo-di-methylation. These epigenetic modifications were involved not only in PPARγ2 expression but also in the adipogenic differentiation potential of osteoporotic BMSCs. Finally, we inhibited osteoporotic BMSC adipogenesis by modulating the patterns of DNA methylation and histone modifications.

2. Results

2.1. The attenuation of osteogenic potential and the enhancement of adipogenic potential of osteoporotic BMSCs

In the current study, a GIO mouse model was established by intraperitoneal injection of Dex for 3 weeks as previously described [45,46]. Saline-injected mice were used as controls and defined as "normal". Micro-CT analysis showed reduced trabecular bone in the proximal tibia (Fig. 1A), including lower bone volume, trabecular number and thickness and higher trabecular space (Fig. 1B). BMSCs were isolated from the bone marrow and cultured in vitro. Flow cytometry analysis revealed that mesenchymal surface markers CD44, CD105 and CD90 were positive (Fig. 1C) and hematopoietic surface markers CD45 and CD34 were negative in these cells (Fig. 1C). BMSCs are induced to osteogenesis in vitro. At week 1, ALP staining analysis revealed that ALP activation was weaker in osteoporotic BMSCs compared with normal BMSCs (Fig. 1D). At week 3, Alizarin Red staining analysis revealed the same pattern as ALP staining (Fig. 1D). The total RNA was extracted at week 2 and used for quantitative RT-PCR analysis for several osteogenic markers Runx2, ALP, BSP and OC. The qRT-PCR revealed the less significant BMP2-induced activation of Runx2, ALP, BSP and OC mRNA expression in osteoporotic BMSCs than normal BMSCs (Fig. 1E). These results indicated that osteoporotic BMSCs had weaker osteogenic potential compared with normal BMSCs.

Alternatively, BMSCs were induced to adipogenesis in vitro. At week 3, fat droplet generation was evaluated by Oil red O staining and quantification. As shown in Fig. 1F, more intracellular fat droplets were observed in osteoporotic BMSCs compared with normal BMSCs. At both weeks 0 and 1, total RNA was harvested for qRT-PCR using primers for adipogenic markers PPARγ2, C/EBPα, and glut4. The qRT-PCR revealed the more significant activation of PPARγ2, C/EBPα, and glut4 mRNA expression in osteoporotic BMSCs than normal BMSCs (Fig. 1G). Further, upon in vitro adipogenic induction, the phosphorylation of PPARγ was greater in osteoporotic BMSCs compared with normal BMSCs (Fig. S1). Together, these lines of evidence suggested that osteoporotic BMSCs had stronger adipogenic potential compared with normal BMSCs.

2.2. PPARγ2 promoter DNA hypomethylation in osteoporotic BMSCs

After observing the increased adipogenic potential of osteoporotic BMSCs, we attempted to elucidate the underlying molecular mechanisms. Our attention is focused on PPARγ2 in the current study. We analyzed the mouse PPARγ2 promoter, which contains six CpG sites (i.e., potential DNA methylation targets) around the transcription start site (TSS) (Fig. 2A): −437 bp, −298 bp, −263 bp, −247 bp, −60 bp, and +89 bp. The DNA sequence was shown in Fig. S2. The methylation statuses of these six CpG sites were investigated in normal and osteoporotic BMSCs with and without adipogenic induction. In the absence of adipogenic induction, PPARγ2 promoter DNA hypomethylation was observed in osteoporotic BMSCs compared with normal BMSCs (Fig. 2B). Similarly, osteoporotic BMSCs from GIO mice exhibited significant DNA hypomethylation upon 3-week adipogenic induction (Fig. 2B). We also performed ChIP assays to measure MeCP2 binding. MeCP2 specifically binds to the DNA methylation sites in the PPARγ2 −446 to −208 bp promoter region that contains four CpG sites in normal and osteoporotic BMSCs with and without adipogenic induction. IgG was used as negative control. Without adipogenic induction, MeCP2 binding in osteoporotic BMSCs was weaker than in normal BMSCs, although the difference was not significant (Fig. 2C). In contrast, upon adipogenic induction, substantially weaker MeCP2 binding was observed in osteoporotic BMSCs (Fig. 2C).

To further analyze PPARγ2 promoter methylation in osteoporotic BMSCs, we investigated the timing of promoter methylation in BMSCs in glucocorticoid-induced osteoporosis. BMSCs were isolated from bone marrow at weeks 0–6 following Dex or saline injection. BMSC

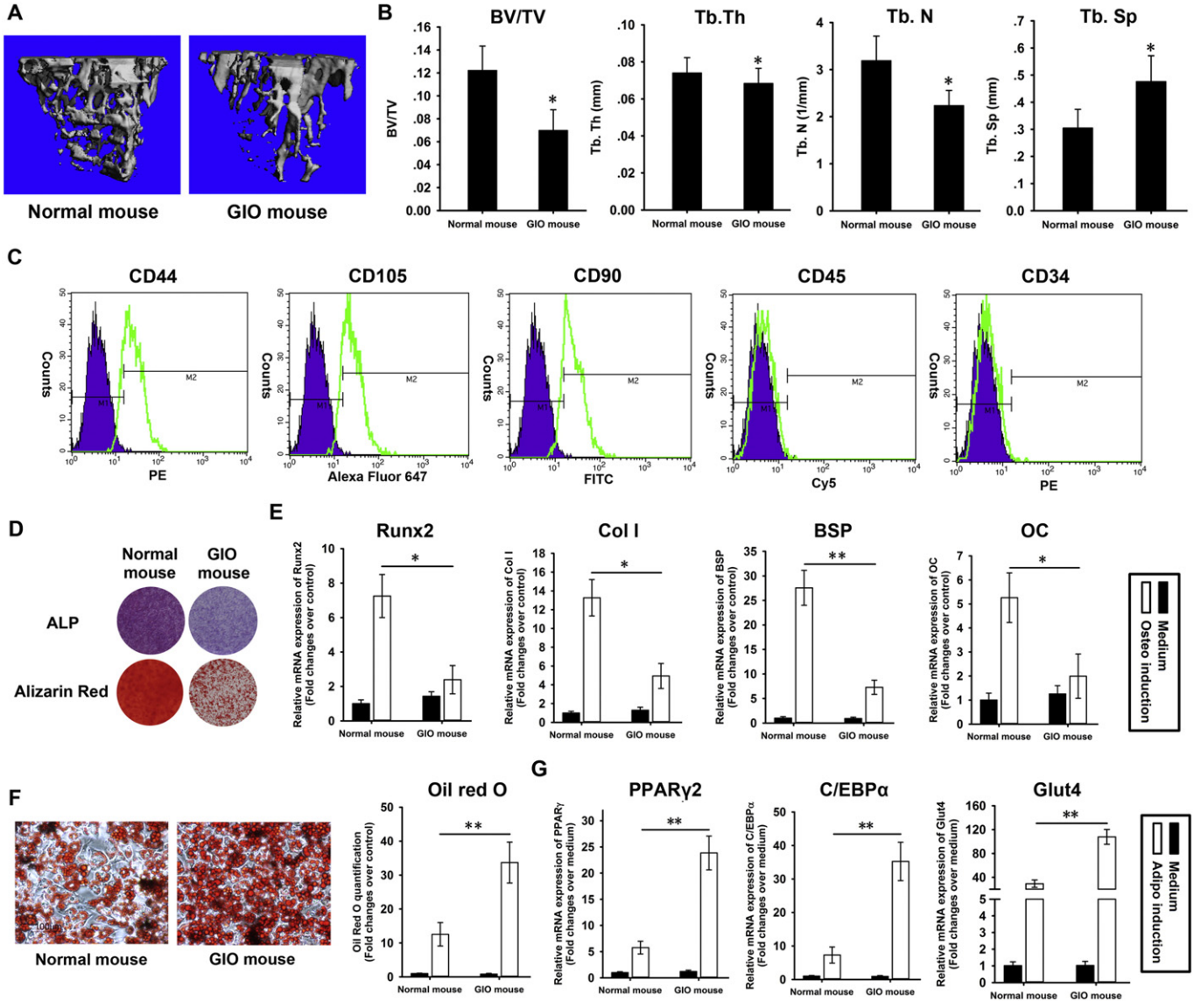

Fig. 1. The attenuation of osteogenic potential and the enhancement of adipogenic potential of osteoporotic BMSCs. A glucocorticoid-induced osteoporosis (GIO) mouse model was established by intraperitoneal injection of Dex (n = 8) or saline (n = 7) for 3 weeks. Micro-CT was employed to investigate the trabecular bone in the proximal tibia (A). BV/TV, trabecular thickness, trabecular number and trabecular space were analyzed (B). BMSCs were isolated from the bone marrow, cultured in vitro and analyzed by flow cytometry for mesenchymal surface markers CD44, CD105 and CD90 and hematopoietic surface markers CD45 and CD34 (C). Then they were induced to undergo osteogenesis. Alkaline phosphatase (ALP) staining and Alizarin red staining were performed at weeks 1 and 3, respectively (D). At week 2, the total RNA was extracted and used for real-time PCR analysis with primers for Runx2, ALP, BSP and OC (E). β-Actin was used as an internal control. BMSCs were induced to adipogenesis. At week 3, fat droplet generation was evaluated by Oid red O staining and quantification (F). At 0 and 1 weeks, total RNA was harvested for quantitative RT-PCR using primers for PPARγ2, C/EBPα, and glut4 (G). HPRT was used as an internal control. The results are expressed as the fold change relative to normal BMSCs without induction. Data are shown as the mean ± SD. *: $p < 0.05$, **: $p < 0.01$. All the data were obtained from at least three independent experiments.

bisulfite-converted PPARγ2 promoter amplicons were digested with *Hpy*CH4IV and the level of demethylation was estimated by the cutting efficiency (see Materials and methods section for details). We detected a gradual demethylation of the PPARγ2 promoter following dexamethasone injection until reaching a plateau at weeks 5 and 6 (Fig. 2D). In contrast, PPARγ2 promoter demethylation in normal BMSCs remained relatively low from weeks 0 to 6, and no significant changes were observed (Fig. 2D).

2.3. PPARγ2 promoter DNA methylation regulates PPARγ2 expression

After observing PPARγ2 promoter hypomethylation in osteoporotic BMSCs, we attempted to investigate its effects on PPARγ2 transcription. Normal BMSCs were treated with a DNA methyltransferase inhibitor, 5′-aza (5 μM and 10 μM), to induce DNA hypomethylation. On day 2, total RNA was recovered for quantitative RT-PCR using primers for PPARγ2. This analysis showed that 5′-aza treatment led to an upregulation of PPARγ2 transcription in a dose-dependent manner (Fig. 3A). When BMSCs were treated with both 5′-aza and the adipogenesis induction cocktail, 5′-aza could still cause an upregulation of PPARγ2 transcription in a dose-dependent manner (Fig. 3A). MeCP2 binds to DNA methylation sites specifically to regulate target gene transcription. In the current study, we used siRNA to silence MeCP2 expression in normal BMSCs (Fig. 3B). PPARγ2 transcription was upregulated in response to MeCP2 knockdown (Fig. 3B). Similarly, a significant upregulation in PPARγ2 transcription was also observed in response to MeCP2 knockdown when BMSCs were induced to undergo adipogenesis (Fig. 3B).

Further, the mouse PPARγ2 promoter (−602–+202 bp) was amplified from genomic DNA by PCR and cloned into the pGL3-basic vector (Fig. 3C). M.*Sss*I was utilized to in vitro methylate the PPARγ2 promoter

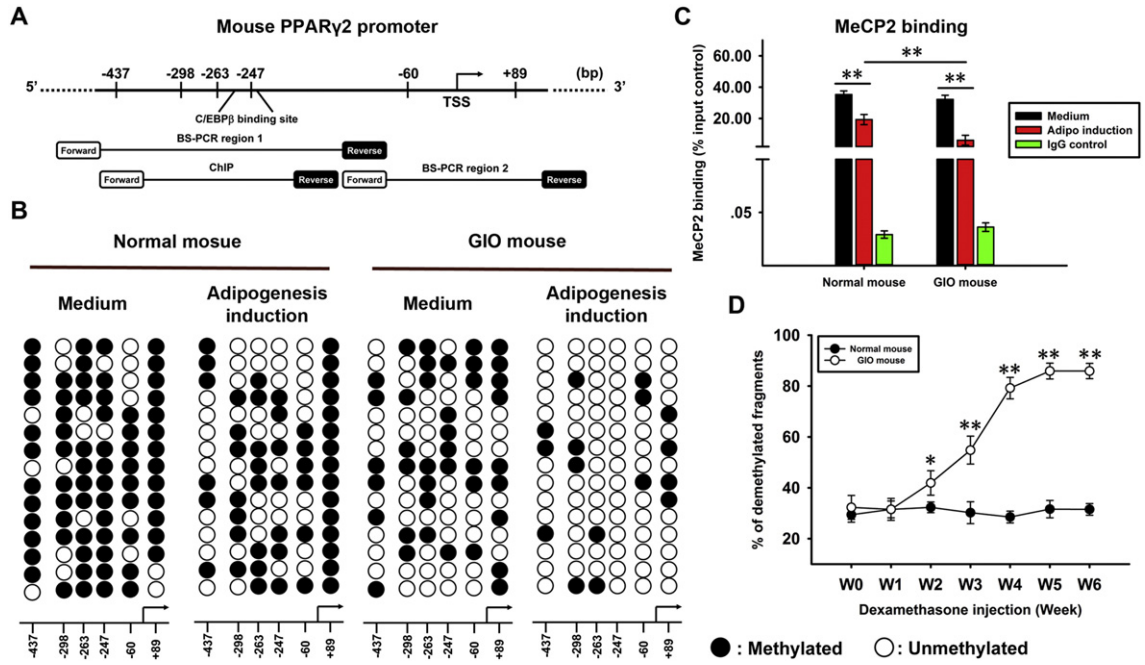

Fig. 2. Osteoporotic BMSC PPARγ2 promoter DNA hypomethylation. Analysis of PPARγ2 promoter DNA methylation and transcription factor binding sites revealed 6 CpG sites and a putative C/EBPβ binding site around the transcription start site (TSS; −258 to −245 bp) (A). Genomic DNA was isolated from normal and osteoporotic BMSCs with and without 3-week adipogenic induction. The DNA methylation statuses of 6 PPARγ2 promoter CpG sites were investigated (B). Open circles indicate unmethylated CpG sites and closed circles indicate methylated CpG sites. ChIP was performed to measure MeCP2 binding to the PPARγ2 promoter in normal and osteoporotic BMSCs with and without adipogenic induction (C). IgG was used as a negative control. The result was expressed as a percentage of MeCP2 binding in input control. Genomic DNA was isolated from normal and osteoporotic BMSCs at 0–6 weeks following Dex injection. The methylation statuses of the −437 bp, −298 bp and −247 bp CpG sites were determined by restriction endonuclease digestion and the fraction of promoter fragments in which all three sites were unmethylated is depicted (D). Data are shown as the mean ± SD. *: $p < 0.05$, **: $p < 0.01$, GIO mouse vs. normal mouse. All the data were obtained from at least three independent experiments.

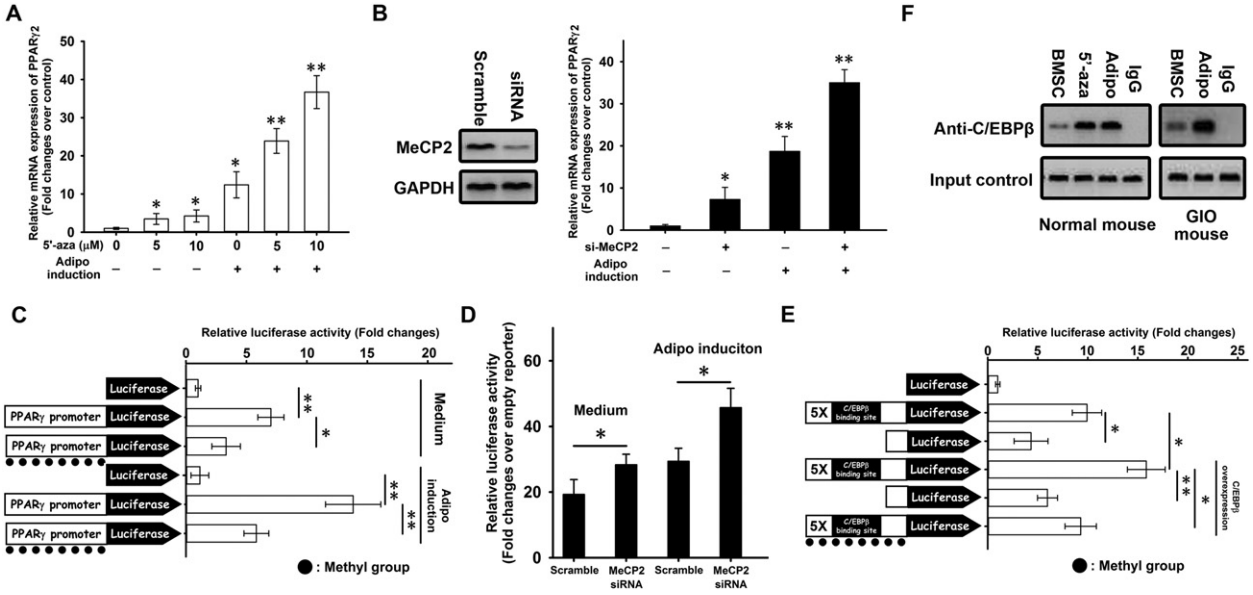

Fig. 3. PPARγ2 promoter DNA methylation regulates PPARγ2 expression. Normal BMSCs were treated with 5′-aza (5 and 10 μM). Total RNA was harvested on day 2 for quantitative RT-PCR using primers for PPARγ2 (A). The results are expressed as the fold change in mRNA abundance relative to "vehicle" culture without adipogenic induction. *: $p < 0.05$, **: $p < 0.01$, vs. "0 μM adipogenic induction (−)" culture. siRNA-mediated knockdown of MeCP2 expression (B). A scrambled siRNA was used as a control. PPARγ2 mRNA expression was measured by quantitative RT-PCR (B). The results are expressed as the fold change in mRNA abundance relative to the "scramble" culture without adipogenic induction. *: $p < 0.05$, **: $p < 0.01$, vs. "scramble adipogenic induction (−)" culture. The mouse PPARγ2 promoter region (−602–+202 bp) was cloned into the pGL3-Basic vector. M.*SssI* was used to methylate CpG sites in vitro, and a transient reporter assay was performed in normal BMSCs with and without adipogenic induction (C). The results are expressed as the fold change in relative luciferase units (RLUs) relative to the "empty reporter" in a medium culture. A transient reporter assay was performed in normal BMSCs with and without MeCP2 knockdown (D). The results are expressed as the fold changes in RLU relative to the "empty reporter" in the scramble culture without adipogenic induction. The PPARγ2 core promoter (−203 –+202 bp) was inserted upstream of the luciferase reporter, and five putative C/EBPβ binding sites were then inserted in tandem upstream of the PPARγ2 core promoter. A transient reporter assay was then performed in normal BMSCs (E). The results are expressed as the fold change in RLU relative to the "empty reporter" culture. Data are shown as the mean ± SD. *: $p < 0.05$, **: $p < 0.01$. ChIP was performed to measure C/EBPβ binding to the PPARγ2 promoter in normal and osteoporotic BMSCs with and without adipogenic induction (F). IgG was used as negative control. All the data were obtained from at least three independent experiments.

and transient reporter assays were then performed in normal BMSCs with and without adipogenic induction. As shown in Fig. 3C, in vitro PPARγ2 promoter methylation resulted in a reduction in luciferase activity. Furthermore, upon adipogenic induction, a reduction in luciferase activity was also observed in response to in vitro methylation (Fig. 3C). A methylated PPARγ2 promoter-driven luciferase vector was transfected into BMSCs with and without MeCP2 knockdown. Transient reporter assays indicated that the luciferase activity of the methylated PPARγ2 promoter was increased in response to MeCP2 knockdown regardless of adipogenic induction (Fig. 3D). Together, these lines of evidence suggest that both DNA methylation and MeCP2 binding are involved in BMSC PPARγ2 transcription.

We noticed a putative C/EBPβ binding site between −258 bp and −245 bp of the PPARγ2 promoter; C/EBPβ is another key transcription factor in adipogenesis (Fig. 2A). Several CpG sites surround this binding site, and a CpG site lies within it (−247 bp); consequently, we were interested in examining the role of C/EBPβ in osteoporotic BMSC expression of PPARγ2. We therefore inserted the PPARγ2 core promoter (−203–+202 bp) upstream of the luciferase reporter, and five putative C/EBPβ binding sites were introduced in tandem upstream of the PPARγ2 core promoter (Fig. 3E). Transient reporter assays were then performed in normal BMSCs. As shown in Fig. 3E, C/EBPβ binding sites significantly enhanced PPARγ2 core promoter luciferase activity. C/EBPβ binding site-driven luciferase reporter activity was further enhanced in response to C/EBPβ overexpression (Fig. 3E). More importantly, luciferase activity was reduced in response to in vitro methylation of the C/EBPβ binding sites despite C/EBPβ overexpression (Fig. 3E).

Finally, we employed ChIP assays to study C/EBPβ binding to the PPARγ2 promoter, and the results indicated that C/EBPβ could indeed bind to that site in both normal and osteoporotic BMSCs (Fig. 3F). And regardless of without or with adipogenic induction, C/EBPβ binding in osteoporotic BMSCs was stronger than in normal BMSCs (Fig. 3F). C/EBPβ binding was enhanced when normal BMSCs were treated with 5′-aza to induce DNA hypomethylation (Fig. 3F), suggesting a negative relationship between DNA methylation and C/EBPβ binding to the PPARγ2 promoter.

2.4. PPARγ2 promoter histone modifications in osteoporotic BMSCs

PPARγ2 promoter histone modifications were also investigated in osteoporotic BMSCs. We first examined the global expression levels of four core histone modifications, acetylated H3K9/K14 and H4K12, di-methylated H3K9 and tri-methylated H3K27, in osteoporotic BMSCs at 0–3 weeks following Dex injection. Total H3 and H4 were used as loading controls. As shown in Fig. 4A, the global levels of all of the histone modifications examined were stable during glucorticoid-induced osteoporosis, suggesting that these histone modifications are not globally affected by osteoporosis.

Histones are important for gene regulation [46]. H3 and H4 tails are heavily acetylated at multiple sites, and these acetylation sites are generally linked to gene activation. In this study, we used ChIP assays to examine the roles of these two histone tails in the PPARγ2 regulatory regions in normal and osteoporotic BMSCs; we selected H3K9/K14 and H4K12 acetylation to represent the acetylation of H3 and H4, respectively. Three regions were examined: 2 kb and 1 kb upstream of the TSS, and the promoter. Primer Chr.15 targets a silent region on mouse chromosome 15 that contains no known genes within 500 kb [38], while the GAPDH primer targets the promoter region of the actively transcribed GAPDH gene. Negative control experiments were performed in parallel using IgG (Fig. S3). We observed significant increases in H3K9/K14 and H4K12 acetylation within the −2 kb, −1 kb and promoter regions in osteoporotic BMSCs compared with normal BMSCs (Fig. 4B and C).

Depending on the site and degree of histone methylation, it can lead to either gene activation or repression. Di-methylated H3K9 and tri-methylated H3K27 are repressive marks although they function through different mechanisms [20,44]. We examined the distribution of these two modifications in PPARγ2 in normal and osteoporotic BMSCs using ChIP analysis. We observed a significant decrease in H3K9 di-methylation in the −2 kb, −1 kb and promoter regions in osteoporotic BMSCs compared with normal BMSCs (Fig. 4D). The PPARγ2 regulatory regions were devoid of H3K27 tri-methylation in both normal and osteoporotic BMSCs, and the two cell types did not differ (Fig. 4E).

Notably, upon adipogenic induction, H3K9/K14 and H4K12 hyperacetylation and H3K9 hypo-di-methylation in PPARγ2 regulatory region were observed in osteoporotic BMSCs compared with normal BMSCs (Fig. S4).

Finally, the binding of phosphorylated RNA polymerase II, a key component of transcription machinery, to the mouse PPARγ2 promoter was investigated using ChIP assays of normal and osteoporotic BMSCs. Without adipogenic induction, p-RNA polymerase II binding did not differ between these cell types (Fig. 4F); in contrast, when adipogenesis was induced, stronger p-RNA polymerase II binding was observed in osteoporotic BMSCs compared with normal BMSCs, suggesting that PPARγ2 transcriptional activity in osteoporotic BMSCs was stronger than in normal BMSCs (Fig. 4F).

2.5. Histone acetylation and H3K9 di-methylation regulate PPARγ2 expression in osteoporotic BMSCs

After observing the increase in histone acetylation and decrease in H3K9 di-methylation in PPARγ2 regulatory regions in osteoporotic BMSCs, we investigated whether these changes affected PPARγ2 expression. We first studied PPARγ2 promoter HDAC1 (responsible for removing histone acetyl groups), LSD1 (responsible for removing methyl groups from H3K9) and SETDB1 (responsible for adding methyl groups to H3K9) occupancy in normal and osteoporotic BMSCs. The ChIP assay results indicated a decrease in HDAC1 and SETDB1 occupancy and an increase in LSD1 occupancy of the PPARγ2 promoter in osteoporotic BMSCs compared with normal BMSCs, regardless of adipogenesis induction (Fig. 5A). These data were consistent with the increases in PPARγ2 H3K9/K14 and H4K12 acetylation and decrease in H3K9 di-methylation in osteoporotic BMSCs (Fig. 4).

Normal BMSCs were treated with TSA, a histone deacetylase inhibitor that causes histone hyper-acetylation, and total RNA was recovered after two days for quantitative RT-PCR analysis of PPARγ2. This assay revealed that TSA could promote PPARγ2 transcription (Fig. 5B); furthermore, when BMSCs were treated with TSA and the adipogenic induction cocktail, TSA continued to promote PPARγ2 transcription (Fig. 5B).

siRNA-mediated silencing of LSD1 led to H3K9 hyper-methylation in osteoporotic BMSCs (Fig. 5C). Without adipogenic induction, PPARγ2 transcription was unaltered in response to LSD1 knockdown (Fig. 5C); in contrast, upon adipogenic induction, PPARγ2 transcription was significantly downregulated in response to LSD1 knockdown (Fig. 5C).

siRNA-mediated silencing of SETDB1 expression led to H3K9 hypomethylation in normal BMSCs (Fig. 5D). A significant increase in PPARγ2 transcription was observed in response to SETDB1 knockdown regardless of adipogenic induction (Fig. 5D).

2.6. The involvement of β-catenin in the epigenetic modifications at PPARγ2 promoter in osteoporotic BMSCs

We then attempted to elucidate the mechanisms underlying DNA hypomethylation, histone hyperacetylation and H3K9 hypo-dimethylation at PPARγ2 promoter in osteoporotic BMSCs. Several reports have indicated that Dex prevents osteoblastogenesis partly by inhibiting the Wnt/β-catenin pathway [32,39,40]. To investigate whether the Wnt/β-catenin pathway is involved in the epigenetic modifications at PPARγ2 promoter in osteoporotic BMSCs, we first evaluated the protein expression of active β-catenin in both normal and osteoporotic BMSCs. The Western blot revealed the lower expression level of active β-catenin in osteoporotic BMSCs compared with normal BMSCs (Fig. 6A). The qRT-PCR results showed the significant downregulation of Wnt target genes Axin2

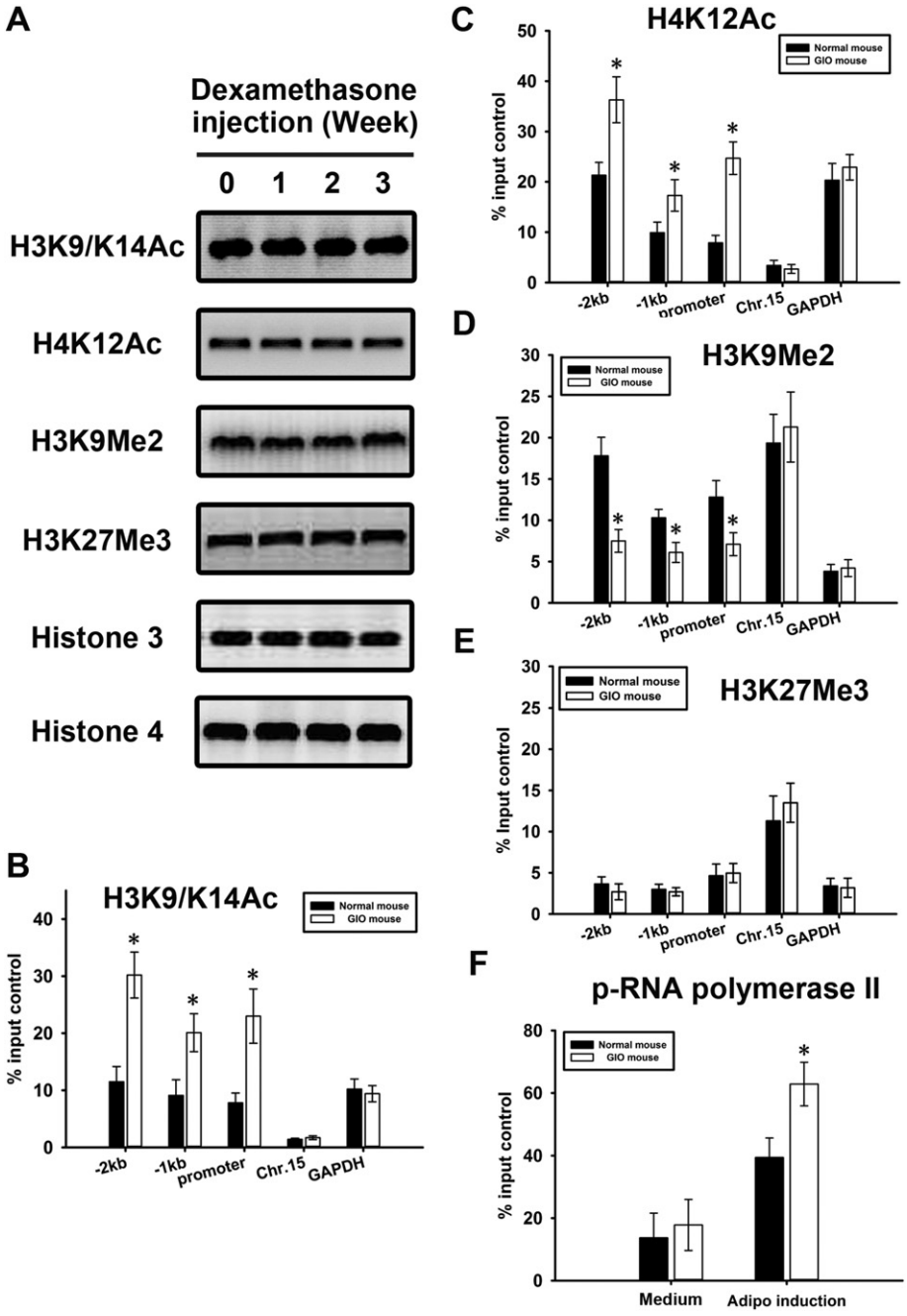

Fig. 4. Histone modifications in osteoporotic BMSC PPARγ2 regulatory regions. Histone samples were collected from osteoporotic BMSCs at 0–3 weeks following Dex injection. Global histone modification levels were determined by Western blot (A). Histones 3 and 4 were used as loading controls. ChIP assays were used to examine acetylated H3K9/K14 (B), H4K12 (C), di-methylated H3K9 (D) and tri-methylated H3K27 (E) occupancy in the PPARγ2 −2 kb, −1 kb and promoter regions in normal and osteoporotic BMSCs. Chromosome 15 and GAPDH were used as negative and positive controls, respectively. Phosphorylated RNA polymerase II occupancy of the PPARγ2 promoter was measured in normal and osteoporotic BMSCs with and without adipogenic induction (F). The results were normalized to the percentage of various histone modifications in the input control. Data are shown as the mean ± SD. *: $p < 0.05$, GIO mouse vs. normal mouse. All the data were obtained from at least three independent experiments.

(Fig. 6B) and cyclin D1 (Fig. 6C) in osteoporotic BMSCs compared with normal BMSCs.

Next, we investigated the functional role of Wnt/β-catenin signal in the establishment of DNA methylation, histone acetylation and methylation at PPARγ2 promoter. IWR-1 was used to block Wnt/β-catenin signal in osteoporotic BMSCs. At day 7, PPARγ2 promoter DNA hypomethylation (Fig. 6D), histone hyper-acetylation (Fig. 6E and F) and H3K9 hypo-dimethylation (Fig. 6G) were observed. Further, LiCl was used to activate Wnt/β-catenin signal in osteoporotic BMSCs. At day 7, PPARγ2 promoter DNA hypermethylation (Fig. 6D), histone hypo-acetylation (Fig. 6E and F) and H3K9 hyper-dimethylation (Fig. 6G) were observed. These results indicated that Wnt/β-catenin signal played an important role in the epigenetic modifications at PPARγ2 promoter in osteoporotic BMSCs.

2.7. The adipogenic differentiation potential of osteoporotic BMSCs is inhibited by altering the patterns of epigenetic modifications

Following the observation of the PPARγ2 epigenetic modification changes in osteoporotic BMSCs and their effects on PPARγ2 expression,

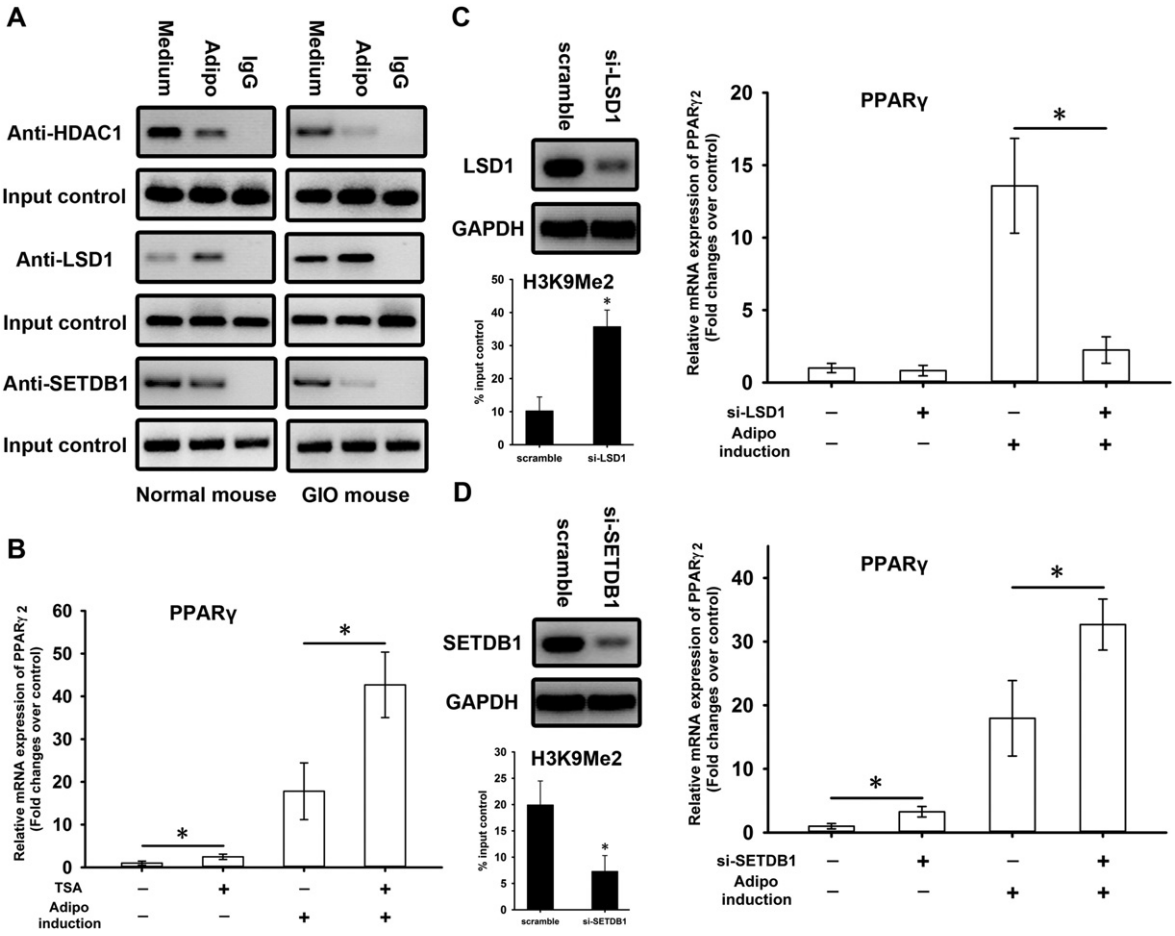

Fig. 5. PPARγ2 promoter histone modifications regulate PPARγ2 expression. ChIP assays were performed to examine HDAC1, LSD1 and SETDB1 occupancy of the PPARγ2 promoter in normal and osteoporotic BMSCs with and without adipogenic induction (A). IgG was used as negative control. Normal BMSCs were treated with TSA (100 nM), and total RNA was harvested on day 2 for quantitative RT-PCR using primers for PPARγ2 (B). The results are expressed as the fold change in mRNA abundance relative to the "vehicle" culture without adipogenic induction. siRNA-mediated knockdown of LSD1 (C) and SETDB1 (D) expression. Scramble was used as control. Di-methylated H3K9 PPARγ2 promoter occupancy was measured by ChIP in response to LSD1 and SETDB1 knockdown (C and D). PPARγ2 mRNA expression was measured by quantitative RT-PCR (C and D). The results are expressed as the fold change in mRNA abundance relative to the "scramble" culture without adipogenic induction. Data are shown as the mean ± SD. *: $p < 0.05$. All the data were obtained from at least three independent experiments.

we attempted to modulate osteoporotic BMSC adipogenic differentiation potential by altering the patterns of epigenetic modifications. We overexpressed Dnmt3a to induce DNA hyper-methylation (Fig. 7A), treated BMSCs with anacardic acid to induce H3K9/K14 (Fig. 7B) and H4K12 (Fig. 7C) hypo-acetylation and overexpressed SETDB1 to induce H3K9 hyper-di-methylation (Fig. 7D) at the PPARγ2 promoter in osteoporotic BMSCs that had been induced to undergo adipogenesis. At week 3, fat droplet generation was evaluated by Oil red O staining and quantification. As shown in Fig. 7E and F, Dnmt3a-overexpression, anacardic acid treatment and SETDB1-overexpression significantly inhibited fat droplet generation in osteoporotic BMSCs. At week 1 after induction, total RNA was harvested for quantitative RT-PCR using primers for PPARγ2, C/EBPα, aP2 and glut4. The mRNA levels of these genes were significantly reduced in response to Dnmt3a-overexpression, anacardic acid treatment and SETDB1-overexpression (Fig. 7G–J) when adipogenesis was induced in osteoporotic BMSCs.

It should be noted that besides PPARγ2, the changes of epigenetic modifications in the regulatory regions of other genes, in response to those epigenetic treatments described above, should not be excluded due to their widespread effects. However, we are sure that PPARγ2 regulatory regions have remarkable sensitivity to those epigenetic treatments, as shown in Fig. 7A–D, and Dnmt3a-overexpression, anacardic acid treatment and SETDB1-overexpression could inhibit the adipogenesis of osteoporotic BMSCs through modulating the epigenetic status of PPARγ2 at least in a large part, if not all.

2.8. The osteogenic differentiation potential of osteoporotic BMSCs is rescued by altering the patterns of epigenetic modifications

Finally, we attempted to modulate osteoporotic BMSCs osteogenic differentiation potential by altering the patterns of epigenetic modifications. We overexpressed Dnmt3a, treated BMSCs with anacardic acid and overexpressed SETDB1 at the PPARγ2 promoter in osteoporotic BMSCs that had been induced to undergo osteogenesis. At week 1, ALP staining analysis revealed that anacardic acid treatment and SETDB1 overexpression could enhance BMP2-induced ALP activity but Dnmt3a overexpression could not (Fig. 8A). At week 3, Alizarin Red staining analysis revealed the same pattern as ALP staining (Fig. 8A). The total RNA was extracted at week 2 and used for qRT-PCR analysis for Runx2, ALP, BSP and OC. The results showed that anacardic acid and SETDB1 overexpression enhanced BMP2-induced Runx2, ALP, BSP and OC activation but Dnmt3a overexpression did not (Fig. 8B–E). These results indicated that the osteogenic differentiation potential of osteoporotic BMSCs was rescued by anacardic acid and SETDB1 overexpression.

3. Discussion

In the current study, a significant enhancement of adipogenic differentiation potential was observed for osteoporotic BMSCs compared with normal BMSCs as measured by the expression of adipogenic

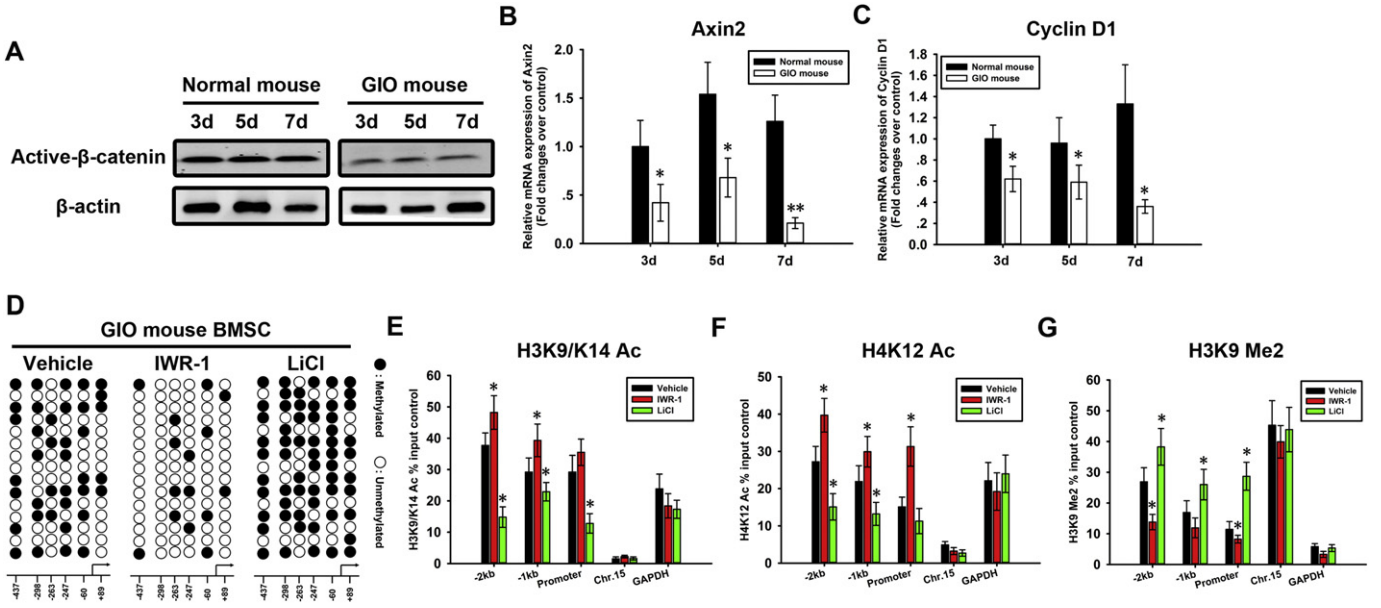

Fig. 6. The involvement of β-catenin in the epigenetic modifications at PPARγ2 promoter in osteoporotic BMSCs. BMSCs were isolated from the bone marrow of normal and osteoporotic mice. Total proteins were harvested for Western blot using antibody against active β-catenin (A). β-Actin was used as loading control. Total RNA was extracted and used for real-time PCR analysis with primers for Axin2 (B) and cyclin D1 (C). β-Actin was used as an internal control. The results were expressed as fold changes relative to "3d" culture of normal BMSCs. IWR-1 (10^{-6} M) and LiCl (20 mM) were used to treat osteoporotic BMSCs. At day 7, genomic DNA was isolated and the DNA methylation statuses of 6 PPARγ2 promoter CpG sites were investigated (D). Open circles indicate unmethylated CpG sites and closed circles indicate methylated CpG sites. ChIP assays were used to examine acetylated H3K9/K14 (E), H4K12 (F) and di-methylated H3K9 (G) occupancy in the PPARγ2 −2 kb, −1 kb and promoter regions in osteoporotic BMSCs treated by IWR-1 and LiCl. Chromosome 15 and GAPDH were used as negative and positive controls, respectively. The results were normalized to the percentage of various histone modifications in the input control. Data are shown as the mean ± SD. *: $p < 0.05$, **: $p < 0.01$. GIO mouse vs. normal mouse, IWR-1 and LiCl vs. vehicle. All the data were obtained from at least three independent experiments.

markers and fat droplet formation, and these results are consistent with a number of previous reports. Previously, researchers identified a remarkable accumulation of adipocytes in the bone marrow from osteoporotic patients compared with healthy elderly subjects, suggesting that bone marrow adipogenesis was involved in osteoporosis pathophysiology. Recently, in vivo proton magnetic resonance (^{1}H MRS) data indicated that increased bone marrow adipogenesis was associated with reduced bone mineral density in patients [1,7,42]. In mice, a complex fat phenotype of mixed brown and white adipose was observed in the bone marrow [13]. Additional work is required to determine whether the quality and quantity of marrow fat plays a functional role in osteoporotic deregulation of bone remodeling.

The potential biological functions and molecular mechanisms underlying osteoporotic BMSC adipogenesis have attracted increasing attention for multiple reasons. First, bone marrow adipocytes were first regarded as structural fillers for the void within the bone marrow cavity; then, these cells were proposed to either store energy or exert biological effects on the adjacent tissues through cytokine production [25] which either sustains or suppresses hematopoietic and osteogenic processes [11,22,24,25]. Second, given that BMSCs are the shared precursor cells for osteoblasts and adipocytes, the osteoporotic phenotype might be rescued by inducing osteoporotic bone marrow adipocyte apoptosis, dedifferentiation to BMSCs, or even transdifferentiation to osteoblasts, which has potential to ameliorate low bone mass in osteoporosis. The current study aimed to elucidate the molecular mechanisms underlying osteoporotic BMSC adipogenesis.

The environment significantly affects bone mass, even during gestation: the intra-uterine environment was shown to play an essential role in fetal skeleton development not only at birth but also later in life. Body weight, fat stores, physical activity and smoking are included as maternal factors affecting neonatal bone mass. Similarly, vitamin D and calcium availability during pregnancy are also closely associated with fetal skeletal development and childhood bone mass. Consequently, it seems that epigenetic influences have a more important role in osteoporosis pathophysiology than genetic factors. The methylation status of the glucocorticoid receptor (GR) and PPARα were reported to be altered in response to maternal dietary restriction in rats, and more importantly, these changes persisted even after weaning and were transmitted to the next generation [15–17]. An increased risk of several metabolic and neurological disorders was reported in Dutch subjects that had experienced famine in 1944, as well as the abnormal methylation status of various gene promoters, such as IGF2 and other genes, that are related to tissue growth and metabolism [8,9]. The current study provides direct evidence that the epigenetic landscape of the PPARγ2 regulatory region is altered in osteoporotic BMSCs, with changes, including DNA hypo-methylation, histone hyper-acetylation and H3K9 hypo-di-methylation, as well as evidence regarding how these epigenetic modifications regulate PPARγ2 expression and osteoporotic BMSC adipogenic differentiation.

In the present study, CpG sites in the PPARγ2 regulatory regions were de-methylated in osteoporotic BMSCs. One CpG site (−247 bp) was included in the C/EBPβ binding site (−258 to −245 bp). We determined that MeCP2 was recruited to these CpG sites when they were hyper-methylated in normal BMSCs, and C/EBPβ was recruited to its binding site when the CpG sites were hypo-methylated in osteoporotic BMSCs. The ChIP data indicated a negative relationship between MeCP2 and C/EBPβ binding to the PPARγ2 promoter (Figs. 2C and 3F). PPARγ2 expression is regulated by C/EBPβ during BMSC adipogenesis. C/EBPβ and C/EBPδ exert their functions in adipocyte differentiation before PPARγ and C/EBPα, and ectopic expression of C/EBPβ in non-adipogenic fibroblasts activates PPARγ and C/EBPα transcription [6]. Furthermore, PPARγ and C/EBPα expression was lost in mouse embryonic fibroblasts (MEFs) obtained from mice lacking both C/EBPβ and C/EBPδ, and these cells were unable to undergo adipogenic differentiation [35]. MeCP2 specifically binds to methylated CpG sites within the genome and provides a platform for the binding of transcriptional activators and repressors. The current study provides insight into the molecular mechanisms underlying how PPARγ2 promoter DNA methylation is linked to MeCP2 and C/EBPβ function to regulate PPARγ2 expression.

In this study, we observed the hyper-acetylation of H3 and H4 tails within the PPARγ2 gene in osteoporotic BMSCs compared with normal

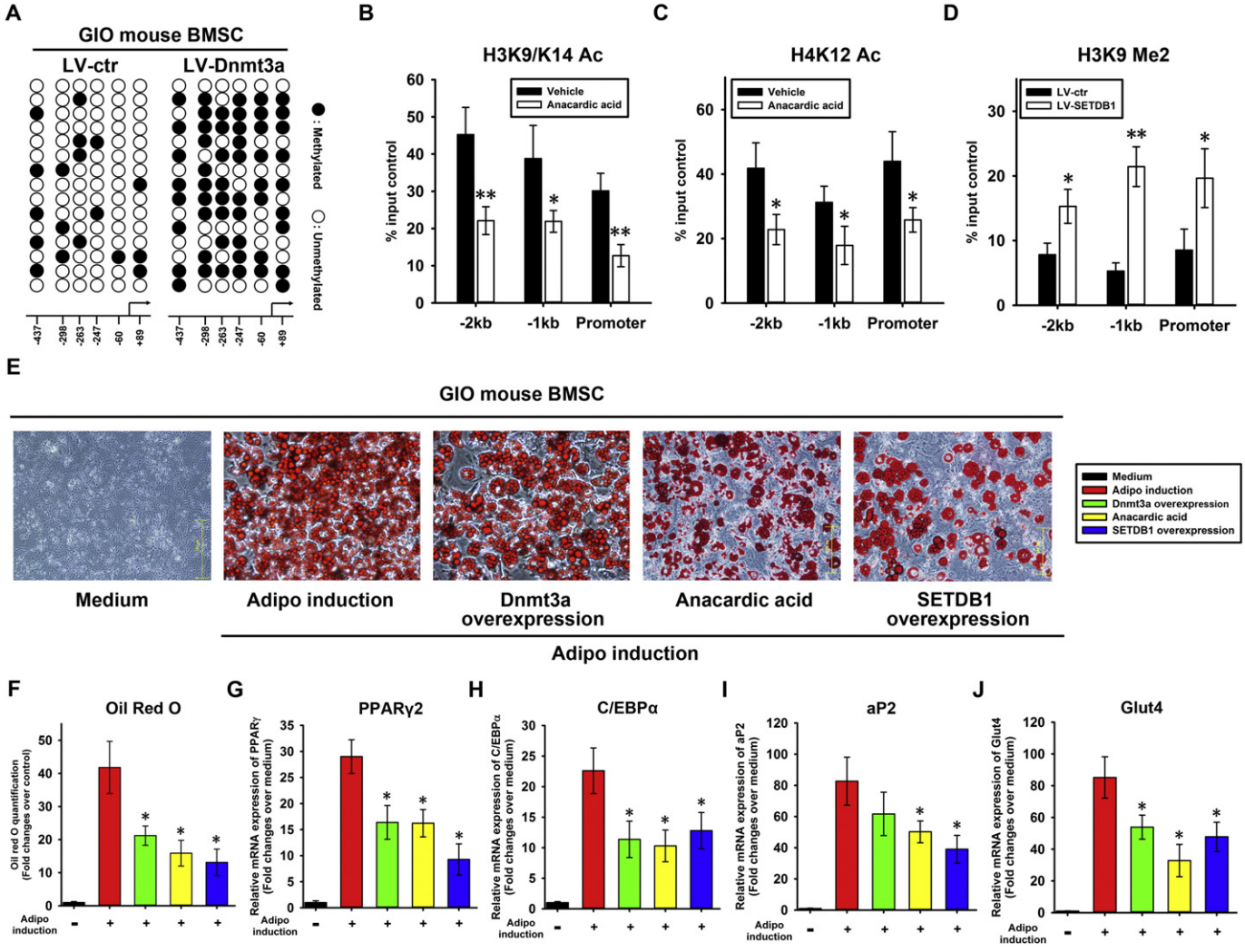

Fig. 7. Osteoporotic BMSC adipogenic differentiation potential is inhibited by alterations in the patterns of epigenetic modifications. Lentiviral overexpression of Dnmt3a and SETDB1 in osteoporotic BMSCs. Osteoporotic BMSCs were treated with anacardic acid (4 μM). The DNA methylation statuses of 6 CpG sites in the PPARγ2 promoter were investigated (A). Open circles indicate unmethylated CpG sites and closed circles indicate methylated CpG sites. ChIP was performed to measure acetylated H3K9/K14 (B), acetylated H4K12 (C) and di-methylated H3K9 (D) PPARγ2 promoter occupancy. The results were normalized to the percentage of various histone modifications in the input control. *: $p < 0.05$, **: $p < 0.01$. Osteoporotic BMSCs overexpressing either Dnmt3a or SETDB1, or treated with anacardic acid were induced to undergo adipogenic differentiation. At week 3, fat droplet generation was evaluated by Oil red O staining (E) and quantification (F). Total RNA was harvested at weeks 0 and 1 for quantitative RT-PCR using primers for PPARγ2 (G), C/EBPα (H), aP2 (I) and glut4 (J). HPRT was used as an internal control. The results are expressed as the fold change relative to the "medium" culture. Data are shown as the mean ± SD. *: $p < 0.05$, vs. adipogenic induction (−). All the data were obtained from at least three independent experiments.

BMSCs (Fig. 4), and this hyper-acetylation enhanced osteoporotic BMSC adipogenic differentiation potential. Our data are supported by previous reports that PPARγ2 promoter H3K9 acetylation is significantly upregulated during adipogenesis [33] and is positively associated with PPARγ2 transcription. Our observations also suggest that HDAC1 is recruited to the PPARγ2 promoter to maintain the hypo-acetylation status of normal BMSCs and is dislodged in osteoporotic BMSCs, leading to hyper-acetylation (Fig. 5). TSA inhibition of HDACs led to PPARγ transcriptional activation (Fig. 5). PPARγ2 gene expression and histone acetylation are closely related. In addition to PPARγ2 promoter histone acetylation, previous reports showed that the lysine (K)-acetyl-transferases (KATs) p300/CBP34 and Tip60 (a MYST family member) [38], which catalyze histone H3 and H4 acetylation, respectively, can bind PPARγ to form heterodimers that activate PPARγ target gene expression. In contrast, SIRT1, a major mammalian HDAC, binds to PPARγ and represses PPARγ target gene expression.

In the current study, we observed PPARγ2 H3K9 hypo-di-methylation in osteoporotic BMSCs compared with normal BMSCs (Fig. 4), which contributed to the enhancement of osteoporotic BMSC adipogenic differentiation potential. These data support earlier reports that H3K9 di-methylation is a marker of inactive chromatin marker. When we used siRNA to silence H3K9 demethylase LSD1, PPARγ2 transcription was repressed, and knockdown of H3K9 methyltransferase SETDB1 produced the opposite result by decreasing H3K9 dimethylation. Our data are consistent with a previous report that the expression of several histone demethylases and methyltransferases was increased during adipogenesis and that H3K4/K9 demethylase LSD1 knockdown resulted in a marked reduction in 3T3-L1 preadipocyte differentiation. Our report and their report differ in that they selected C/EBPα as target gene.

In the current study, we found that Wnt/β-catenin signaling played an important role in the establishment and maintenance of epigenetic modifications of PPARγ2 promoter in osteoporotic BMSCs. This result is supported by a previous study. Li et al. found that the Wnt/β-catenin pathway is involved in Dex-induced osteoporosis and C/EBPα promoter methylation, and its activation by LiCl rescues the effect of Dex on C/EBPα promoter methylation and osteoblast/adipocyte balance [14]. Further, some previous studies indicated that non-canonical Wnt signal induced osteoblastogenesis through PPARγ transrepression

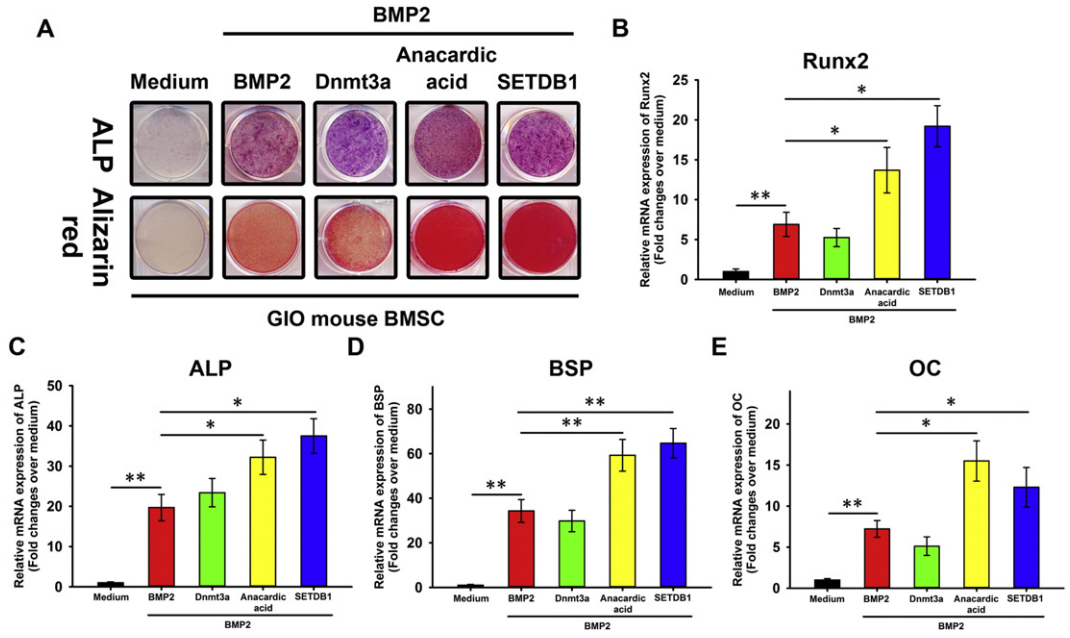

Fig. 8. The osteogenic differentiation potential of osteoporotic BMSCs is rescued by altering the patterns of epigenetic modifications. Osteoporotic BMSCs overexpressing either Dnmt3a or SETDB1, or treated with anacardic acid were induced to undergo osteogenic differentiation. Alkaline phosphatase (ALP) staining and Alizarin red staining were performed at weeks 1 and 3, respectively (A). At week 2, the total RNA was extracted and used for real-time PCR analysis with primers for Runx2 (B), ALP (C), BSP (D) and OC (E). β-Actin was used as an internal control. The results were expressed as fold changes relative to a "medium" culture. *: $p < 0.05$, **: $p < 0.01$. All the data were obtained from at least three independent experiments.

by a histone methyltransferase [34]. These studies suggest Wnt/β-catenin signal as potential target to treat osteoporosis.

In the current study, we attempted to modulate osteoporotic BMSC potential for adipogenic differentiation by altering epigenetic modifications using two methods: gene engineering and treatment with exogenous inhibitors. Dnmt3a-overexpression caused DNA hyper-methylation, anacardic acid treatment caused H3 and H4 tail hypo-acetylation, and SETDB1-overexpression caused H3K9 hyper-di-methylation of PPARγ2 in osteoporotic BMSCs. In response to these treatments, osteoporotic BMSC adipogenic differentiation was significantly inhibited. Investigations into osteoporosis epigenetics may provide not only a deeper insight into osteoporosis pathophysiology but also reveal specific genes as new targets for epigenetics-based osteoporosis therapy. Some anti-methylation agents are already employed to treat tumors [12,28], and perhaps these agents can be used in osteoporosis; however, their widespread effects are some of the most significant detractions limiting their potential utility. Agents that can specifically modulate the epigenetic modifications of certain genes in a given pathway would be of much greater use. In the current study, we obviously cannot exclude the widespread effects of Dnmt3a-overexpression, anacardic acid treatment and SETDB1-overexpression. However, we confirmed that PPARγ2 regulatory regions have remarkable sensitivity to those epigenetic treatments and their overall effects on osteoporotic BMSCs were inhibiting adipogenic differentiation through PPARγ2 at least in a large part, if not all.

In addition, the osteogenic differentiation potential of osteoporotic BMSCs was investigated in response to Dnmt3a overexpression, anacardic acid treatment and SETDB1 overexpression. We found that Dnmt3a overexpression could not enhance the osteogenic differentiation of osteoporotic BMSCs. In a recent study, Nishikawa K et al. identified Dnmt3a as a transcription factor that couples these metabolic changes toosteoclast differentiation. They found that SAM-mediated DNA methylation by Dnmt3a regulates osteoclastogenesis via epigenetic repression of anti-osteoclastogenic genes [21]. Therefore, we speculate that Dnmt3a might regulate bone mass and homeostasis through modulating osteoclastogenesis, but not osteoblastogenesis.

In the current study, we found that anacardic acid treatment and SETDB1 overexpression were effective in the rescue of the osteogenic differentiation of osteoporotic BMSCs. There are rare reports to investigate the role of anacardic acid in BMSC osteogenesis. To our knowledge, the current study is the first one to evaluate its effect on osteogenesis and to confirm that anacardic acid treatment could enhance osteogenic differentiation potential of osteoporotic BMSCs. For SETDB1, previous studies mainly focused its role in the transrepression of PPARγ and the inhibition of adipogenesis [21]. Our current study paid attention to osteogenesis and confirmed that SETDB1 overexpression could rescue the osteogenic differentiation potential of osteoporotic BMSCs. We believe that our study provides deeper insights into the mechanisms of osteoporosis and stronger evidences that SETDB1 can be regarded as a potential target to develop anti-osteoporosis drugs.

In summary, the results of the current study suggest that DNA is demethylated, H3 and H4 tails are acetylated, and H3K9 di-methylation is reduced in PPARγ2 regulatory regions in osteoporotic BMSCs compared with normal BMSCs. These epigenetic modifications lead to an active chromatin structure that activates PPARγ2 transcription in response to adipogenic induction. Consistent with this idea, osteoporotic BMSCs showed enhanced potential for adipogenic differentiation in response to PPARγ2 epigenetic modifications (Fig. 9).

4. Materials and methods

4.1. GIO mouse model

BALB/c mice (7 months old, approximately 25 g bodyweight) were housed in the Shanghai Jiaotong University School of Medicine Animal Facility under standard conditions. The mice were dosed once daily intraperitoneally with saline ($n = 7$) or dexamethasone (Dex) phosphate ($n = 8$) (5 mg/kg; Sigma, St. Louis, MO, USA) for 3 weeks. Throughout the dosing period, the mice were weighed to examine the effects of dosing on body weight. The animals were then sacrificed with an intraperitoneally injected overdose of sodium pentobarbitone. The femurs were removed by dissection for micro-computerized tomography (CT) analysis using Scanco Medical CT-40 instruments. Three dimensional analyses were performed to determine bone volume (BV)/tissue volume (TV), trabecular number (Tb. N), trabecular thickness (Tb. Th), and trabecular separation (Tb. Sp) at the distal femur. The treatment protocol

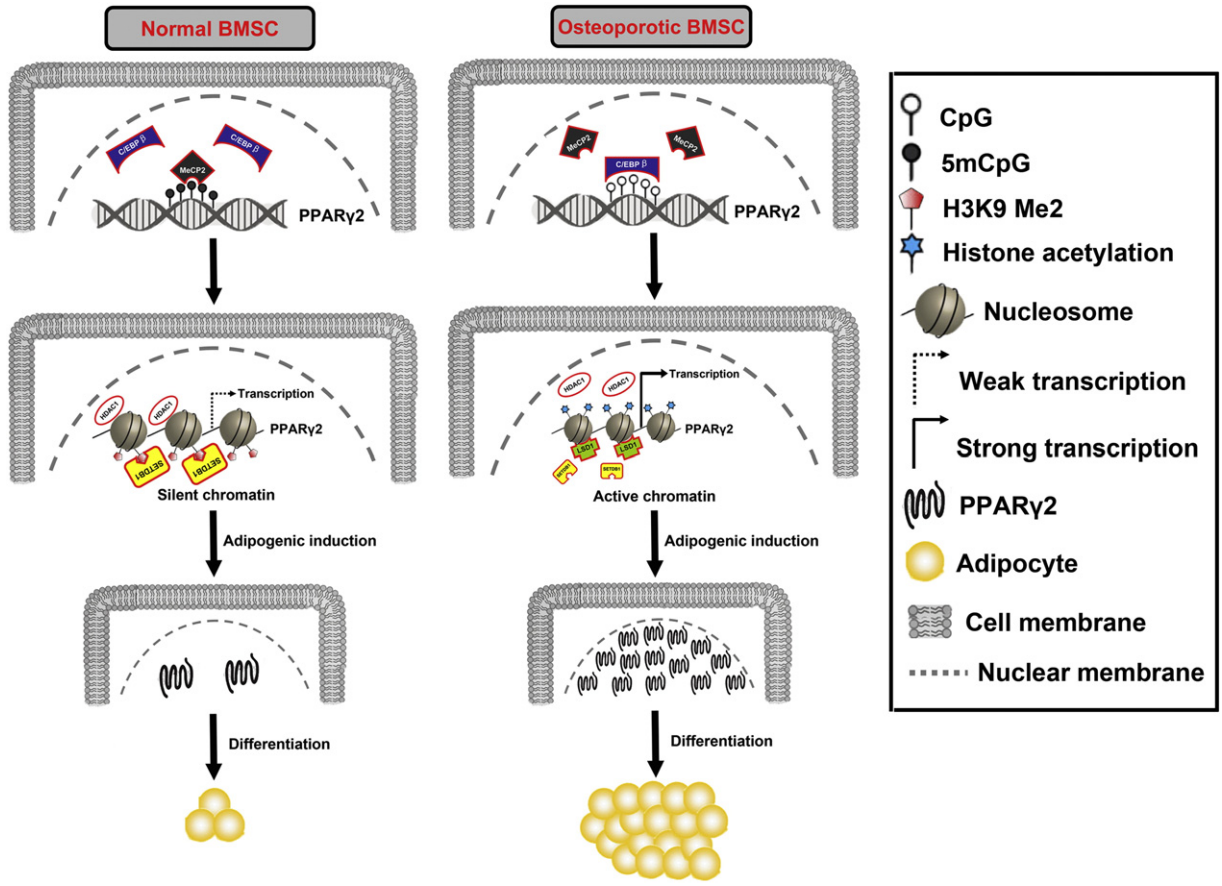

Fig. 9. Epigenetic modifications in the PPARγ2 regulatory region contribute to the enhancement of osteoporotic BMSC potential for adipogenic differentiation. The PPARγ2 regulatory region DNA was de-methylated, H3 and H4 tails were acetylated, and H3K9 di-methylation was reduced in osteoporotic BMSCs compared with normal BMSCs. These epigenetic modifications led to an active chromatin structure that activated PPARγ2 transcription in response to adipogenic induction. Consequently, the adipogenic differentiation potential of osteoporotic BMSCs was enhanced.

was approved by the Ethics Committee and the Animal Research Committee of Shanghai Jiaotong University School of Medicine.

4.2. BMSC isolation, culture, treatment and adipogenic differentiation

Tibia and femur bones were stripped of muscle and placed in ice cold PBS supplemented with 2% fetal bovine serum (FBS, Gibco by Invitrogen, Carlsbad, CA, USA). The epiphyseal ends were then removed and the bones were centrifuged at 4000 *g* for 1 min in a microfuge tube. The bone marrow cells were then suspended in ice cold PBS supplemented with 2% FBS, passed through a 70 μm filter and counted with a hemocytometer.

Filtered bone marrow cells were suspended in PBS containing 2% FBS and 0.1 g/L phenol red and then enriched for lineage negative (Lin−) cells using the SpinSep system (Stem Cell Technologies, Vancouver, BC, Canada). The cells were incubated with a murine progenitor enrichment cocktail (anti-CD5, anti-CD45R, anti-CD11b, anti-Gr-1, anti-TER119, and anti-7/4; Stem Cell Technologies) on ice for 30 min, washed, and then incubated with dense particles on ice for 20 min. The cells were then layered on a density medium, centrifuged at 1200 *g* for 10 min, and the cells at the density medium/PBS interface were collected, washed and counted.

Enriched bone marrow cells were seeded onto culture plates at a density of 0.1×10^6 cells/cm^2 in murine Mesencult media (Stem Cell Technologies) containing 100 units/ml penicillin (Gibco), 100 μg/ml streptomycin (Gibco) and 0.25 μg/ml amphotericin B (Gibco). The media were changed after 48 h and adherent cells were maintained in culture with twice weekly media changes.

BMSCs were treated with 5 and 10 μM 5′-aza (Sigma), 100 nM trichostatin A (TSA) (Sigma), 10^{-6} M Dex, 10^{-6} M IWR-1, 20 mM LiCl and 4 μM anacardic acid (Sigma).

To induce osteogenic differentiation, BMSCs were treated with BMP-2 (R&D Systems, Minneapolis, MN, USA) at final concentrations of 150 ng/ml.

Adipogenic differentiation was induced as previously described [4]; briefly, confluent cells were fed with a complete adipogenic hormone cocktail (DMEM supplemented with 10% FBS, 10 g/ml of insulin (Sigma), 0.5 mM methylisobutylxanthine (MIX) (Sigma) and 1 μM Dex (Sigma)). The start point of differentiation was referred to as day 0. On day 3, cells were fed with DMEM containing only insulin and 10% FBS. On day 6, complete adipogenic hormone cocktail was again added.

4.3. ALP staining and Alizarin Red staining

A previously described protocol was employed [45]. Cultured cells were rinsed with a phosphate-buffered saline (PBS) three times and fixed with 4% paraformaldehyde for 10 min at 4 °C. The fixed cells were soaked in 0.1% naphthol AS-MX phosphate (Sigma) and 0.1% fast red violet LB salt (Sigma) in 56 mM 2-amino-2-methyl-1,3-propanediol (Sigma) for 10 min at room temperature, washed with PBS, and then observed under a digital camera.

Osteoblast maturation was examined by staining mineralized nodules with Alizarin Red. After fixation, the cells were washed with PBS and soaked in 40 mM Alizarin Red (pH 4.2) for 30 min at 37 °C, then washed with PBS and imaged.

4.4. Fat quantization by Oil red O staining

The cells were fixed with 10% formalin for 1 h and then stained in pre-warmed Oil red O solution for 1 h in a 60 °C water bath. The red-stained lipid droplets were observed under a light microscope. To measure the quantification of lipid accumulation, Oil red O was eluted by adding 100% isopropanol and optical density was detected using a spectrophotometer at 520 nm.

4.5. Reverse transcription (RT)-PCR and real-time PCR

Total RNA was isolated from BMSCs using an RNeasy Mini Kit (Qiagen, Valencia, CA, USA) according to the manufacturer's protocol. For RT-PCR, single-stranded cDNA was reverse-transcribed from 1 μg of total RNA using reverse transcriptase and an oligo-dT primer. PCR was performed with 1 μl of cDNA using the following cycling parameters: 30 cycles of 94 °C for 40 s, 60 °C for 40 s, and 72 °C for 40 s. The PCR products were then analyzed by agarose gel electrophoresis. Quantitative PCR was performed using a 96-well-plate ABI Prism 7500 (Applied BioSystems, Foster City, CA, USA) and SYBR Green PCR Master Mix (Takara Bio Inc., Otsu, Japan). Cycling conditions were as follows: 94 °C for 30 s followed by 40 cycles of 94 °C for 5 s and 60 °C for 34 s. The comparative $2^{-\Delta\Delta Ct}$ method was used to calculate the relative expression of each target gene. Glyceraldehyde-3-phosphate dehydrogenase (GAPDH) was used as an internal control for RT-PCR and hypoxanthine guanine phosphoribosyl transferase (HPRT) was used as an internal control for quantitative RT-PCR. Primer sequences used in RT-PCR were listed in Table S1. Primer sequences used in quantitative RT-PCR were used in Table S2.

4.6. Western blot

Histone preparations from BMSCs at different time points during glucocorticoid-induced osteoporosis were prepared as previously described [29]. Total proteins from BMSCs treated by Dex at different time points were prepared. Equal amounts of proteins were resolved by 15% SDS-PAGE, transferred onto PVDF membranes and probed with antibodies recognizing non-phospho (active) β-catenin (Cell Signaling Technology, Danvers, MA, USA), H3K9/K14 acetylation, H4K12 acetylation and H3K27 tri-methylation (Upstate, New York, NY, USA), and H3K9 di-methylation, total H3 and total H4 (Abcam, Cambridge, MA, USA).

4.7. DNA isolation and bisulfite sequencing PCR

Briefly, 5 μg genomic DNA was cut with EcoRI at 37 °C overnight and then purified using NaOAc and absolute alcohol. The purified DNA was denaturated for 15 min at 50 °C with 5.5 μl of 2 M NaOH. Two volumes of 2% low-melting agarose were then added to the DNA solution and agarose beads were formed by pipetting 10 μl aliquots of the DNA/agarose mixture into cold mineral oil. Freshly prepared hydroxyquinone (55 μl of 10 mM; Sigma) and sodium bisulfite (520 μl 40.5%, pH 5; Sigma) were added, and the mixture was incubated under mineral oil at 50 °C for 16 h. Modification was completed by treatment with NaOH (0.3 M final concentration) for 10 min at room temperature.

PCR amplifications were performed in 20 μl reactions containing one agarose/DNA bead and 2 units of rTaq polymerase (Takara). The primer sequences were as follows: BS-PCR region 1, 5′-GATGTGTGATTAGGAG TTTTAA-3′ (forward) and 5′-ACTATCTACTACTTTAACAAAA-3′ (reverse); and BS-PCR region 2, 5′-ACACACCATTTTGTCACAACTG-3′ (forward) and 5′-AATAAACCAAAATAACATCTCT-3′ (reverse). The amplified PCR fragments were gel-purified and cloned into the pMD19-T vector system (Takara). Fifteen clones were sequenced per sample and the sense strands were used to assess CpG site methylation.

For restriction enzyme digestion analysis, PCR products corresponding to BS-PCR region 1, site −437 bp and site −247 bp were digested with *Hpy*CH4IV (New England Biolabs, Ipswich, Massachusetts, USA) and electrophoresed to separate the digested fragments (for region 1 fragments, at least one of −437 bp, and −247 bp was methylated) and undigested fragments (for region 1 fragments, all of the four CpG sites were unmethylated). The bisulfite reaction only converts unmethylated cytosine residues to thymine and PCR fragments generated from unmethylated genomic DNA are resistant to *Hpy*CH4IV digestion. The relative levels of the digested and undigested fragments were estimated following analysis of images of ethidium bromide stained agarose gels using Quantity One™ software.

4.8. Chromatin immunoprecipitation (ChIP)

Cells were cross-linked with 1% formaldehyde for 10 min at 37 °C and crude nuclei were purified using a previously described protocol [29]. The crude nuclei were sonicated to produce chromatin fragments of approximately 500 bp. The antibodies used in the ChIP assay were as follows: MeCP2, C/EBPβ, histone 3, H3K9 di-methylation, HDAC1, and phospho-RNA polymerase II (Abcam); and H3K9/K14 acetylation, H4K12 acetylation, and H3K27 tri-methylation (Upstate). Rabbit IgG (Sigma) was included as a negative control. For each ChIP assay, 2–5 μg of antibodies was added and the samples were incubated overnight at 4 °C. The ChIP and input DNA samples were quantified by quantitative PCR. For PPARγ2, primers targeting the regions 2 kb (−2 kb) and 1 kb (−1 kb) upstream of the transcription start site (TSS) were used. Promoter primers were designed to be within 500 bp upstream of the TSS. Primer sequences used in ChIP-qPCR were listed in Table S3.

4.9. Lentivirus

Lentiviral vectors containing the coding sequences of C/EBPβ, DNA methyltransferase 3A (Dnmt3a), and SETDB1, and short interfering (si)RNAs against MeCP2, LSD1 and SETDB1 were purchased from Genecopoeia® (Rockville, MD, USA). Virus particles were generated as previously described [5]. Briefly, $1.3–1.5 \times 10^6$ 293 T cells were plated in a 10 cm dish and the transfection mixture was added directly to the culture medium at 70–80% confluence. Following transfection, the samples were incubated in a CO_2 incubator at 37 °C for 48 h and the virus particle-containing medium was then collected.

4.10. Luciferase reporter assay

Cells were seeded into 24-well plates. All plasmids for transfection were isolated using a Qiagen plasmid purification kit (Qiagen). Transient transfections were performed using Lipofectamine 2000 (Invitrogen) according to the manufacturer's instruction; phRL-SV40 vector (Promega, Madison, WI, USA) was used as control for transfection efficiency. Forty-eight hours after transfection, both firefly and *Renilla* luciferase activities were measured using a Dual-luciferase reporter assay system (Promega) and a Luminoskan TL plus Luminometer (MTX Labsystems, Vienna, VA, USA) according to the manufacturer's protocol. The relative luciferase units (RLUs), the ratios of firefly to *Renilla* luciferase activities, were then obtained.

4.11. In vitro methylation assay

M.*Sss*I (New England Biolabs, Ipswich, MA, USA) (2 U/μg DNA) was used to in vitro methylate CpG sites for 6 h at 37 °C and then inactivated at 65 °C for 15 min. Treated DNA fragments and vectors were ligated and purified by phenol/chloroform extraction and ethanol precipitation. The plasmid concentrations were determined by measuring the absorbance at 260 nm.

4.12. Statistical analysis

Statistical significance was calculated using Student's t-test for two-sample comparisons and one-way ANOVA for multiple comparisons in SPSS 16.0 software. Tukey's test was applied to identify significant differences by ANOVA. Statistical significance was determined using data from at least three independent experiments, and p values of <0.05 were defined as significant. All data are presented as the mean $\pm$ SD unless otherwise specified.

Conflicts of interest

None.

Transparency document

The Transparency document associated with this article can be found, in the online version.

Acknowledgments

This study was supported by grants from the National Natural Science Foundation of China (81000778 and 81370050) and the Municipal Natural Science Foundation of Shanghai (No. 14ZR1433100).

Appendix A. Supplementary data

Supplementary data to this article can be found online at http://dx.doi.org/10.1016/j.bbadis.2015.08.020.

References

[1] G.M. Blake, J.F. Griffith, D.K. Yeung, P.C. Leung, I. Fogelman, Effect of increasing vertebral marrow fat content on BMD measurement, T-score status and fracture risk prediction by DXA, Bone 44 (2009) 495–501.
[2] Z. Cao, R.M. Umek, S.L. McKnight, Regulated expression of three C/EBP isoforms during adipose conversion of 3T3-L1 cells, Genes Dev. 5 (1991) 1538–1552.
[3] M. Esteller, Cancer epigenetics for the 21st century: what's next? Genes Cancer 2 (2011) 604–606.
[4] Q. Fan, T. Tang, X. Zhang, K. Dai, The role of CCAAT/enhancer binding protein (C/EBP)-alpha in osteogenesis of C3H10T1/2 cells induced by BMP-2, J. Cell. Mol. Med. 13 (2009) 2489–2505.
[5] Q.M. Fan, B. Yue, Z.Y. Bian, W.T. Xu, B. Tu, K.R. Dai, G. Li, T.T. Tang, The CREB–Smad6–Runx2 axis contributes to the impaired osteogenesis potential of bone marrow stromal cells in fibrous dysplasia of bone, J. Pathol. 228 (2012) 45–55.
[6] S.R. Farmer, Transcriptional control of adipocyte formation, Cell Metab. 4 (2006) 263–273.
[7] J.F. Griffith, D.K. Yeung, G.E. Antonio, F.K. Lee, A.W. Hong, S.Y. Wong, E.M. Lau, P.C. Leung, Vertebral bone mineral density, marrow perfusion, and fat content in healthy men and men with osteoporosis: dynamic contrast-enhanced MR imaging and MR spectroscopy, Radiology 236 (2005) 945–951.
[8] B.T. Heijmans, E.W. Tobi, L.H. Lumey, P.E. Slagboom, The epigenome: archive of the prenatal environment, Epigenetics 4 (2009) 526–531.
[9] B.T. Heijmans, E.W. Tobi, A.D. Stein, H. Putter, G.J. Blauw, E.S. Susser, P.E. Slagboom, L.H. Lumey, Persistent epigenetic differences associated with prenatal exposure to famine in humans, Proc. Natl. Acad. Sci. U. S. A. 105 (2008) 17046–17049.
[10] T. Kouzarides, Chromatin modifications and their function, Cell 128 (2007) 693–705.
[11] A. Krings, S. Rahman, S. Huang, Y. Lu, P.J. Czernik, B. Lecka-Czernik, Bone marrow fat has brown adipose tissue characteristics, which are attenuated with aging and diabetes, Bone 50 (2012) 546–552.
[12] N.B. La Thangue, Histone deacetylase inhibitors and cancer therapy, J. Chemother. 16 (Suppl. 4) (2004) 64–67.
[13] B. Lecka-Czernik, Marrow fat metabolism is linked to the systemic energy metabolism, Bone 50 (2012) 534–539.
[14] J. Li, N. Zhang, X. Huang, J. Xu, J.C. Fernandes, K. Dai, X. Zhang, Dexamethasone shifts bone marrow stromal cells from osteoblasts to adipocytes by C/EBPalpha promoter methylation, Cell Death Dis. 4 (2013) e832.
[15] K.A. Lillycrop, E.S. Phillips, A.A. Jackson, M.A. Hanson, G.C. Burdge, Dietary protein restriction of pregnant rats induces and folic acid supplementation prevents epigenetic modification of hepatic gene expression in the offspring, J. Nutr. 135 (2005) 1382–1386.
[16] K.A. Lillycrop, E.S. Phillips, C. Torrens, M.A. Hanson, A.A. Jackson, G.C. Burdge, Feeding pregnant rats a protein-restricted diet persistently alters the methylation of specific cytosines in the hepatic PPAR alpha promoter of the offspring, Br. J. Nutr. 100 (2008) 278–282.
[17] K.A. Lillycrop, J.L. Slater-Jefferies, M.A. Hanson, K.M. Godfrey, A.A. Jackson, G.C. Burdge, Induction of altered epigenetic regulation of the hepatic glucocorticoid receptor in the offspring of rats fed a protein-restricted diet during pregnancy suggests that reduced DNA methyltransferase-1 expression is involved in impaired DNA methylation and changes in histone modifications, Br. J. Nutr. 97 (2007) 1064–1073.
[18] L.J. Melton III, How many women have osteoporosis now? J. Bone Miner. Res. 10 (1995) 175–177.
[19] E.J. Moerman, K. Teng, D.A. Lipschitz, B. Lecka-Czernik, Aging activates adipogenic and suppresses osteogenic programs in mesenchymal marrow stroma/stem cells: the role of PPAR-gamma2 transcription factor and TGF-beta/BMP signaling pathways, Aging Cell 3 (2004) 379–389.
[20] M.M. Musri, M.C. Carmona, F.A. Hanzu, P. Kaliman, R. Gomis, M. Parrizas, Histone demethylase LSD1 regulates adipogenesis, J. Biol. Chem. 285 (2010) 30034–30041.
[21] K. Nishikawa, Y. Iwamoto, Y. Kobayashi, F. Katsuoka, S. Kawaguchi, T. Tsujita, T. Nakamura, S. Kato, M. Yamamoto, H. Takayanagi, et al., DNA methyltransferase 3a regulates osteoclast differentiation by coupling to an S-adenosylmethionine-producing metabolic pathway, Nat. Med. 21 (2015) 281–287.
[22] Y. Omatsu, T. Sugiyama, H. Kohara, G. Kondoh, N. Fujii, K. Kohno, T. Nagasawa, The essential functions of adipo-osteogenic progenitors as the hematopoietic stem and progenitor cell niche, Immunity 33 (2010) 387–399.
[23] S.H. Ralston, B. de Crombrugghe, Genetic regulation of bone mass and susceptibility to osteoporosis, Genes Dev. 20 (2006) 2492–2506.
[24] J.P. Rodriguez, P. Astudillo, S. Rios, A.M. Pino, Involvement of adipogenic potential of human bone marrow mesenchymal stem cells (MSCs) in osteoporosis, Curr. Stem Cell Res. Ther. 3 (2008) 208–218.
[25] C.J. Rosen, C. Ackert-Bicknell, J.P. Rodriguez, A.M. Pino, Marrow fat and the bone microenvironment: developmental, functional, and pathological implications, Crit. Rev. Eukaryot. Gene Expr. 19 (2009) 109–124.
[26] C.J. Rosen, M.L. Bouxsein, Mechanisms of disease: is osteoporosis the obesity of bone? Nat. Clin. Pract. Rheumatol. 2 (2006) 35–43.
[27] H. Santos-Rosa, C. Caldas, Chromatin modifier enzymes, the histone code and cancer, Eur. J. Cancer 41 (2005) 2381–2402.
[28] F.P. Santos, H. Kantarjian, G. Garcia-Manero, J.P. Issa, F. Ravandi, Decitabine in the treatment of myelodysplastic syndromes, Expert. Rev. Anticancer. Ther. 10 (2010) 9–22.
[29] D. Shechter, H.L. Dormann, C.D. Allis, S.B. Hake, Extraction, purification and analysis of histones, Nat. Protoc. 2 (2007) 1445–1457.
[30] A. Shilatifard, Chromatin modifications by methylation and ubiquitination: implications in the regulation of gene expression, Annu. Rev. Biochem. 75 (2006) 243–269.
[31] D. Shoback, Update in osteoporosis and metabolic bone disorders, J. Clin. Endocrinol. Metab. 92 (2007) 747–753.
[32] E. Smith, B. Frenkel, Glucocorticoids inhibit the transcriptional activity of LEF/TCF in differentiating osteoblasts in a glycogen synthase kinase-3beta-dependent and -independent manner, J. Biol. Chem. 280 (2005) 2388–2394.
[33] D.J. Steger, G.R. Grant, M. Schupp, T. Tomaru, M.I. Lefterova, J. Schug, E. Manduchi, C.J. Stoeckert Jr., M.A. Lazar, Propagation of adipogenic signals through an epigenomic transition state, Genes Dev. 24 (2010) 1035–1044.
[34] I. Takada, M. Suzawa, K. Matsumoto, S. Kato, Suppression of PPAR transactivation switches cell fate of bone marrow stem cells from adipocytes into osteoblasts, Ann. N. Y. Acad. Sci. 1116 (2007) 182–195.
[35] T. Tanaka, N. Yoshida, T. Kishimoto, S. Akira, Defective adipocyte differentiation in mice lacking the C/EBPbeta and/or C/EBPdelta gene, EMBO J. 16 (1997) 7432–7443.
[36] P. Tontonoz, E. Hu, B.M. Spiegelman, Stimulation of adipogenesis in fibroblasts by PPAR gamma 2, a lipid-activated transcription factor, Cell 79 (1994) 1147–1156.
[37] P. Tontonoz, B.M. Spiegelman, Fat and beyond: the diverse biology of PPARgamma, Annu. Rev. Biochem. 77 (2008) 289–312.
[38] O. van Beekum, A.B. Brenkman, L. Grontved, N. Hamers, N.J. van den Broek, R. Berger, S. Mandrup, E. Kalkhoven, The adipogenic acetyltransferase Tip60 targets activation function 1 of peroxisome proliferator-activated receptor gamma, Endocrinology 149 (2008) 1840–1849.
[39] F.S. Wang, J.Y. Ko, D.W. Yeh, H.C. Ke, H.L. Wu, Modulation of Dickkopf-1 attenuates glucocorticoid induction of osteoblast apoptosis, adipocytic differentiation, and bone mass loss, Endocrinology 149 (2008) 1793–1801.
[40] F.S. Wang, C.L. Lin, Y.J. Chen, C.J. Wang, K.D. Yang, Y.T. Huang, Y.C. Sun, H.C. Huang, Secreted frizzled-related protein 1 modulates glucocorticoid attenuation of osteogenic activities and bone mass, Endocrinology 146 (2005) 2415–2423.
[41] W.C. Yeh, Z. Cao, M. Classon, S.L. McKnight, Cascade regulation of terminal adipocyte differentiation by three members of the C/EBP family of leucine zipper proteins, Genes Dev. 9 (1995) 168–181.
[42] D.K. Yeung, J.F. Griffith, G.E. Antonio, F.K. Lee, J. Woo, P.C. Leung, Osteoporosis is associated with increased marrow fat content and decreased marrow fat unsaturation: a proton MR spectroscopy study, J. Magn. Reson. Imaging 22 (2005) 279–285.
[43] M. Zayzafoon, W.E. Gathings, J.M. McDonald, Modeled microgravity inhibits osteogenic differentiation of human mesenchymal stem cells and increases adipogenesis, Endocrinology 145 (2004) 2421–2432.
[44] Q. Zhang, M.K. Ramlee, R. Brunmeir, C.J. Villanueva, D. Halperin, F. Xu, Dynamic and distinct histone modifications modulate the expression of key adipogenesis regulatory genes, Cell Cycle 11 (2012) 4310–4322.
[45] Y.X. Zhang, H.L. Sun, H. Liang, K. Li, Q.M. Fan, Q.H. Zhao, Dynamic and distinct histone modifications of osteogenic genes during osteogenic differentiation, J. Biochem. (2015).
[46] Q.H. Zhao, S.G. Wang, S.X. Liu, J.P. Li, Y.X. Zhang, Z.Y. Sun, Q.M. Fan, J.W. Tian, PPARgamma forms a bridge between DNA methylation and histone acetylation at the C/EBPalpha gene promoter to regulate the balance between osteogenesis and adipogenesis of bone marrow stromal cells, FEBS J. 280 (2013) 5801–5814.